



Year: 2017

Discovery of Open Cubane Core Structures for Biomimetic LnCo₃(OR)4 Water Oxidation Catalysts

Schilling, Mauro ; Hodel, Florian H ; Luber, Sandra

Abstract: Bio-mimetic catalysts such as LnCo₃(OR)4 (Ln=Er, Tm; OR=alkoxide) cubanes have recently been in the focus of research for artificial water oxidation processes. Previously, the remarkable adaptability with respect to ligand shell, nuclear structure as well as protonation and oxidation states of those catalysts has been shown to be beneficial for the water oxidation process. We further explored the structural flexibility of those catalysts and present here a series of novel structures in which one metal center is pulled out of the cubane cage. This leads to an open cubane core, which is to some extent reminiscent of observed open/closed cubane-core forms of the oxygen-evolving complex in nature's photosystem II. We investigate how those open cubane core models alter the thermodynamics of the water oxidation cycle and how different solvation approaches influence their stability.

DOI: <https://doi.org/10.1002/cssc.201701527>

Posted at the Zurich Open Repository and Archive, University of Zurich
ZORA URL: <https://doi.org/10.5167/uzh-143471>
Journal Article
Accepted Version

Originally published at:
Schilling, Mauro; Hodel, Florian H; Luber, Sandra (2017). Discovery of Open Cubane Core Structures for Biomimetic LnCo₃(OR)4 Water Oxidation Catalysts. *ChemSusChem*, 10(22):4561-4569.
DOI: <https://doi.org/10.1002/cssc.201701527>

Discovery of open cubane-core Structures for bio-mimetic $\{\text{LnCo}_3(\text{OR})_4\}$ Water Oxidation Catalysts

Mauro Schilling^[a], Florian H. Hodel^[a] and Sandra Luber^{*[a]}

Abstract: Bio-mimetic catalysts such as $\{\text{LnCo}_3(\text{OR})_4\}$ ($\text{Ln} = \text{Er}, \text{Tm}$, OR = alkoxide) cubanes have recently been in the focus of research for artificial water oxidation processes. Previously, the remarkable adaptability with respect to ligand shell, nuclear structure as well as protonation and oxidation states of those catalysts has been shown to be beneficial for the water oxidation process. We further explored the structural flexibility of those catalysts and present here a series of novel structures in which one metal center is pulled out of the cubane cage. This leads to an open cubane core, which is to some extend reminiscent of observed open/closed cubane core forms of the oxygen-evolving complex in nature's photosystem II. We investigate how those open cubane core models alter the thermodynamics of the water oxidation cycle and how different solvation approaches influence their stability.

Introduction

In the field of artificial water splitting, nature's oxygen-evolving complex (OEC), which is embedded in a large complex of proteins forming the so-called photosystem II, serves as a leading paradigm for the development of efficient water oxidation catalysts (WOCs). The oxo-bridged cuboidal core formed by three manganese metal centers and a redox-inert calcium ion, as well as a fourth, so called 'dangling' manganese of the OEC cluster (CaMn_4O_5) has inspired the development of numerous artificial water oxidation catalysts. Even though molecular Mn-oxide catalysts mimicking the structural features of the OEC haven been successfully synthesized, they display no significant WOC activity.^[1] Other mimics such as Co(III)-cubanes^[2] need to be carefully scrutinized because catalytically active CoO_x nanoparticles might form in decomposition reactions or their catalytic activity might stem from Co(II) impurities in the sample.^[3] The current lack of understanding regarding the mechanistic principles governing the catalytic activity of elaborate synthetic OEC models calls for further explorations of cubane-type WOCs, among which Co(II)-based cubanes are promising candidates. The first biomimetic WOC based on a Co(II)-cubane motif, $[\text{Co}_4(\text{hmp})_4(\mu_1\text{-OAc})_2(\mu_2\text{-OAc})_2(\text{H}_2\text{O})_2]$ (hmp = 2-(hydroxymethyl)-pyridine) $\{\text{Co}_4(\text{OR})_4\}$, was reported by *Evangelisti et al.* in 2013.^[4] In a subsequent study, by introducing a redox inert Ln^{3+} cation mimicking Ca^{2+} and slightly changing the ligand environment, they matched the structural features of the OEC even more closely and measured significantly higher turnover frequencies (maximum values of 9 s^{-1} compared to 5 s^{-1} at pH 9^[4,5]).

Computational methods are an important tool to gain further insight, which is a prerequisite for the informed design of efficient WOCs^[6]. Over the past years they have been successfully applied to a variety of Co(III)-cubane based catalysts and model systems. Among them are the well-known Co(III)-cubanes by *Dismukes* and co-workers^[2] which have been further modified by organic ligand framework.^[7] EPR measurements suggesting the existence of a $\{\text{Co}(\text{III})_3\text{Co}(\text{VI})\}$ state were supported by computational results,^[8] and the proposed di-oxo state prior to the oxygen-oxygen bond formation was characterized by both spectroscopic methods and Kohn-Sham density functional theory (DFT).^[9] In order to rationalize isotopic labeling studies, ligand exchange reactions were modeled by *Dismukes*, *De Angelis*, and co-worker leading to a possible cis-gemdiol intermediate as a prerequisite for the oxygen-oxygen bond formation^[10]. *Li* and *Siegbahn* modeled the catalytic cycle of a model Co(III)-cubane (without any organic ligands) as well as the Co(III)-cubane of *Dismukes* and co-workers where they found a water nucleophilic attack (WNA) to be favorable in both cases.^[11] The mechanisms of similar model systems were also investigated in great detail by *Wang* and *Van Voorhis*^[12] using a mixed quantum mechanics / molecular mechanics approach as well as by *Fernando* and *Aikens* who found a radical coupling mechanism to be energetically favorable.^[13] In previous studies we investigated ligand-exchange reactions, possible catalytic states and mechanisms of both $\{\text{Co}_4(\text{OR})_4\}$ and $\{\text{LnCo}_3(\text{OR})_4\}$ ($\text{Ln} = \text{Er}, \text{Tm}$) cubanes (see Figure 1; due to ligand exchange,^[5] the ground state structures used for the computational study are not identical to the X-ray structures) using DFT and DFT-based molecular dynamics (MD). Aside from an oxo-oxo coupling mechanism which involves two metal centers, a possible water oxidation pathway of these WOCs is a single-site mechanism involving four consecutive proton coupled electron transfer (PCET) steps at the same metal center and a WNA producing molecular oxygen as well as 4 protons and 4 electrons.

The first PCET step transforms $\text{Co}^{1\text{II}}(\text{OH}_2)\text{OH}$ (S0) into $\text{Co}^{1\text{III}}(\text{OH})_2$ (S1) (see Figure 1). Then, depending on the site of deprotonation one of the two possible oxyl/oxo-species $\text{Co}^{1\text{IV}}(\text{O})\text{OH}$ (S2) is formed. Next, a nucleophilic water attack takes place forming the O-O bond followed by another PCET resulting in a hydroperoxo species $\text{Co}^{1\text{III}}(\text{OOH})\text{OH}$ (S3). Release of the fourth proton and electron produces $\text{Co}^{1\text{III}}(\text{OO})\text{OH}$ (S4) which has (similar to S2) significant radical character on the ligand. Finally,

molecular oxygen is released and the catalyst returns to its ground state by taking up a water molecule from the solvent. In our previous studies we highlighted the importance of flexibility in terms of structural changes of the cubane core during the catalytic cycle, the capability of the catalyst to undergo ligand exchange reactions, and the redox isomerism that allows the catalyst to redistribute electrons over the entire cubane core, all of which potentially enable or even enhance the water oxidation

[a] MSc. M. Schilling, Dr. F. H. Hodel, Prof. Dr. S. Luber
Department of Chemistry C
University of Zurich
Winterthurerstrasse 190
E-mail: sandra.luber@chem.uzh.ch

Supporting information for this article is given via a link at the end of the document

capability.^[14] Thereby, in particular the Co1-O1 and Co1-O2 bonds were found to be prone to distortions. In this work, we set out to further explore this phenomenon. Starting from the formerly reported “distorted” cubane core structures (see Figure 1),^[14] additional local minima on the potential energy surface were located where the structures feature Co1-O1 and Co1-O3 bonds which are even more elongated (see Figure 1). In the following, we discuss the thermodynamics of water oxidation catalyzed by these “open” cubane core structures.

Methods

We employed the same methods as previously applied to $\{ErCo_3(OR)_4\}$, $\{TmCo_3(OR)_4\}$ and $\{Co_4(OR)_4\}$ ^[5,14,15]. For a detailed justification of the computational settings, we ask the reader to review the mentioned literature. The geometries of the “distorted” closed conformers were optimized using the QUICKSTEP program^[16] as implemented in the CP2K software package^[17] employing the BP86 exchange-correlation density functional.^[18] Electronic energies were obtained from single point energy calculations on the BP86 optimized structures using the B3LYP hybrid density functional.^[19] The BP86 functional has been shown to accurately reproduce molecular structures of transition metal complexes.^[20] However, in order to obtain accurate electronic energies the use of hybrid exchange-correlation functionals is required, as has been shown by Kwapien et al.^[21] The use of hybrid functionals such as B3LYP, which include exact Hartree-Fock exchange, generally overstabilizes high spin configurations.^[22] However, counter-examples were found among the catalytic intermediates of $\{ErCo_3(OR)_4\}$, $\{TmCo_3(OR)_4\}$ and $\{Co_4(OR)_4\}$.^[14,15] The initial atomic coordinates of the S0 state were obtained from a snapshot of a DFT-based MD trajectory where all water molecules except for the 68 closest to the catalyst were deleted. The structures for the S1-S4 states were subsequently generated from their respective previous state to ensure that the solvent molecules were in comparable positions.^[14,15] For this work only one of the two possible configurational isomers of the S2 state is of importance (isomer b^[14]) since no open cubane core structures were found for the other isomer. We thus will not distinguish between them in the remaining part of the manuscript. Single point energy calculations were performed on both the geometry optimized system including the catalyst surrounded by 68 water molecules and the catalyst with the same structure but without explicit solvent molecules. All calculations using CP2K were performed in a 30^3 Å^3 simulation box, applying mixed Gaussian and plane wave basis sets with (scalar-relativistic) Goedecker-Teter-Hutter pseudopotentials,^[5,23] double- ζ valence polarized basis sets (DZVP-MOLOPT-GTH^[24] for O, H, N and C, DZVP-MOLOPT-SR-GTH^[24] for Co, as well as newly fitted basis sets for Er and Tm^[5]). Further, Grimme’s D3 dispersion correction was used for all calculations.^[25] The energy cutoff for the auxiliary plane wave expansion of the charge density was set to 500 Ry. Due to the lack of experimental data, ferromagnetic coupling between the Co and Ln centers was assumed for all catalytic states. The proposed mechanism only involves one active Co center, and alterations of the electronic configurations were exclusively performed at this center. The geometries of all intermediates were optimized for all reasonable spin multiplicities. Then, the electronic structures were analyzed in terms of Mulliken spin populations and frontier (canonical) orbitals. Mulliken spin populations depend on the basis set and in general do not converge to the basis set limit,^[26] still they have been routinely used.^[21,27]

The differences in free energy between the catalytic intermediates and the ground state ΔG_{i-0} were calculated following a protocol by Nørskov et al.^[28] that has already been successfully applied to the Co(II)-based cubanes and other catalysts.^[14,15,29] This approach is based on the assumption that all oxidation processes are coupled to deprotonations (PCETs) and that these reactions are essentially barrier free. Hence, contributions of the proton and the electron are not treated independently. ΔG_{i-0} is calculated as

$$\Delta G_{Si-S0} = \left(E_{Si} + \frac{i}{2} E_{H_2} - E_{S0} \right) + \left(E_{ZPE,Si} + \frac{i}{2} E_{ZPE,H_2} - E_{ZPE,S0} \right) + i(\Delta H - T\Delta S), \quad i = 1, \dots, 4$$

E_i is the electronic energy of state i , and $E_{ZPE,i}$ is the zero-point-energy. The thermal corrections for the different intermediates of the catalysts were assumed to cancel out. Therefore, only correction terms for molecular hydrogen containing $\Delta S = 0.016 \frac{\text{kcal}}{\text{K mol}}$ as well as $\Delta H = 1.153 \frac{\text{kcal}}{\text{mol}}$, i.e. half the entropy and enthalpy of molecular hydrogen at standard conditions, are included.^[30]

The computations of the minimum electronic energy paths and barriers with explicit solvation and the CP2K package were carried out with the nudged elastic band (NEB) method^[31] (improved tangent method^[32], climbing image NEB every 5 steps), each pathway consisting of 8 frames. Due to computational cost, we employed only the BP86 functional for these calculations, all other set-up parameters being identical to the ones chosen for the geometry optimizations. For all frames along the optimized reaction pathway electronic energies were obtained employing the B3LYP functional. The zero-point energies were obtained from normal mode analysis in the harmonic approximation. Due to the high computational effort, such calculations were performed in TURBOMOLE 7.01^[33] with the conductor-like screening model (COSMO)^[34] instead of explicit solvation. In order to investigate the effects of the explicit solvation shell, all structures optimized in CP2K (with explicit solvation) were re-optimized in TURBOMOLE using COSMO and no explicit water molecules. It is important to note that the novel conformers would not have been detected without the appropriate initial geometries obtained from CP2K including the explicit first solvation shell. The geometries were optimized using the BP86 exchange-correlation density functional, Ahlrich’s def2-TZVP^[35] basis set, a scalar-relativistic effective core potential (ECP-28) on Er and Tm, respectively, and the resolution-of-the-identity-density-fitting technique^[36] with corresponding auxiliary basis sets,^[37] as well as Grimme’s D3 correction. Single point electronic energies were obtained using the B3LYP hybrid functional but otherwise unchanged settings. For all minimum electronic energy structures, normal mode analysis using the NUMFORCE^[38] script were

performed to confirm that the structures represent minima on the potential energy surface. The COSMO energies were further refined using the direct-COSMO-RS (DCOSMO-RS) procedure as implemented in TURBOMOLE based on the provided σ -potential files for water at 25°C.^[39] Geometry optimizations carried out for a few selected structures using DCOSMO-RS were virtually identical with the structures obtained using COSMO. However, recently DCOSMO-RS was reported to significantly improve activation and reaction energies of organic reactions in protic solvent.^[40] The two-center shared electron numbers (SENs) were calculated via population analysis based on occupation numbers as implemented in TURBOMOLE.^[41] The kinetic barrier for the cubane core opening was evaluated by calculating an approximate reaction path for this process employing the WOELFLING script with standard settings as defined by TURBOMOLE.^[42] Molecular structures were visualized using VMD^[43] or CYLview.^[44]

Results and Discussion

In our previous work we reported an energetically possible “distorted” conformation for the S2 state of $\{\text{LnCo}_3(\text{OR})_4\}$ ^[14] (see Figure 1). Those structures sparked our interest since they might be part of a different catalytic cycle than the one presented in Ref. ^[14]. We therefore investigated this phenomenon further. Starting from the previously described structures, we found even more distorted structures – for the sake of brevity in the following referred to as “open” structures in contrast to “closed” ones featuring a closed cubane core - which can be used to build a complete catalytic cycle in a consecutive manner. The open structures represent minima on the potential energy surface and exhibit elongated Co1-O1 and Co1-O3 bonds that cause Co1 to change its coordination geometry from octahedral to tetrahedral (see Figure 1). The larger Co1-O distances allow the water ligand of Co1 to form an intramolecular hydrogen bond with O1, that further stabilizes the structure. The open cage motif is reminiscent of observations made for the OEC, which is also known to form open and closed cubane core structures.^[45,46] Moreover, the reduction of the coordination number is similar to a recent postulation of a five-fold coordinated Mn(IV) intermediate in the water oxidation reaction catalyzed by the OEC.^[47] However, it is important to note that the open/closed conformers of the OEC and $\{\text{LnCo}_3(\text{OR})_4\}$ are significantly different. In the case of the OEC, an oxygen atom is pulled-out of the cubane cage by the dangling manganese opening up the cubane core. The catalysts at hand, $\{\text{LnCo}_3(\text{OR})_4\}$, do not possess a fourth redox-active transition metal center, further the oxygen atoms which form the cubane core are a fundamental part of the hmp ligand and therefore restricted in their spatial movement. The covalent linkage of those oxygen atoms to carbon backbone of the ligands is the main reason why we do not expect their involvement in the oxygen-oxygen bond formation process, as considered for other model catalysts.^[13] In contrast to the OEC where the bridge-site oxygen's can be protonated,^[48] no such involvement can be found for $\{\text{LnCo}_3(\text{OR})_4\}$ because they are coordinately saturated. Additionally a geminal oxo-oxyl coupling pathway can be excluded since a cis-dioxocobalt center would be a prerequisite for such a pathway.^[10,49] Existence of such a species is questionable due to the requirement of a high oxidation state.

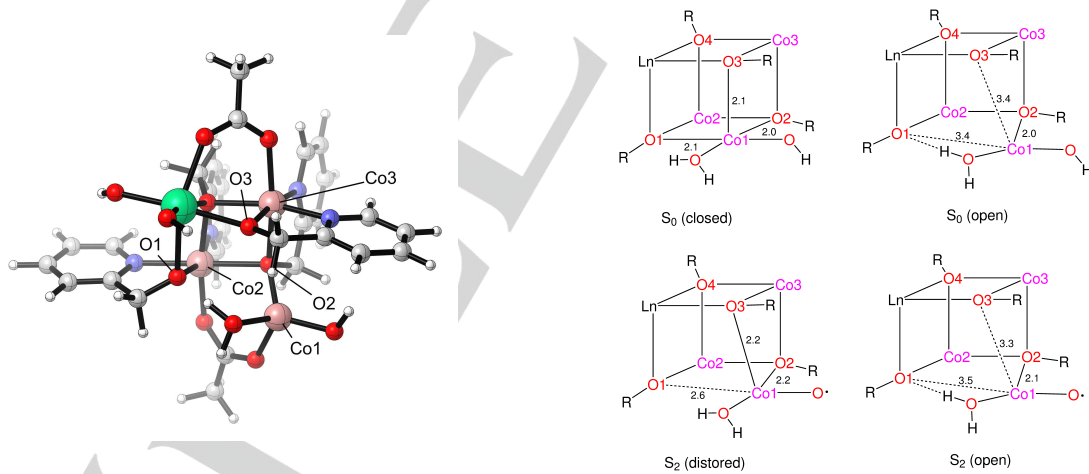


Figure 1. Left: Open cubane core structure of $\{\text{LnCo}_3(\text{OR})_4\}$ in the S0 state used in this study. The cobalt centers as well as some key oxygen atoms are labeled. Note that the ligand framework is identical to the one used in our previous study,^[14] but not to the reported crystal structure due to ligand exchange.^[5] Right: Schematic representation of the open and closed cubane core structures of $\{\text{LnCo}_3(\text{OR})_4\}$ in the catalytic ground state S0 (top). In particular, the Co1-O1 and Co1-O3 bonds are significantly elongated in the former. The same is true when comparing the distorted and open conformers of intermediate S2 (bottom). Distances are given in Å.

Possible water oxidation pathways based on a WNA mechanism are given in Figure 2. In the inner circle, water oxidation catalyzed by the known closed structures is visualized. The outer circle represents the open forms newly presented in this manuscript. We find the open structure of the ground state (S0) to be thermodynamically more stable than the closed one, as indicated by the difference in zero-point corrected electronic energy. This trend is reversed for the first intermediate (S1) where the closed structure is more stable. However, the energy difference is less than 5 kcal/mol, which indicates - given a sufficiently low energetic barrier in between - that the open and closed structures potentially coexist. For the S0 and S1 states, both catalysts $\{\text{ErCo}_3(\text{OR})_4\}$ and $\{\text{TmCo}_3(\text{OR})_4\}$ show a comparable behavior. An exception to this trend is the second intermediate (S2) where the open structure is

thermodynamically more stable in case of $\{\text{ErCo}_3(\text{OR})_4\}$ while $\{\text{TmCo}_3(\text{OR})_4\}$ clearly favors the closed structure. The difference can be rationalized by comparing some selected bond lengths, namely Co1-O1, Co1-O2, and Co1-O3. The latter are within 0.1 Å of one another, when comparing structures of $\{\text{ErCo}_3(\text{OR})_4\}$, and $\{\text{TmCo}_3(\text{OR})_4\}$ optimized with the same spin multiplicity (see Tables S9 and S10 in SI). However, a low spin configuration on Co1 has been found to be energetically favored in the case of $\{\text{ErCo}_3(\text{OR})_4\}$, which is not the case for $\{\text{TmCo}_3(\text{OR})_4\}$ (vide infra; see Table S8 in SI). For the latter, an intermediate spin state is energetically preferred where the Co1-O3 bond is elongated by 0.3 Å compared to the low spin state. The elongation of the bond results in complete breakage as can be seen from the reduction of the SEN from $\sigma_{\text{Co1-O3}} = 0.13$ to $\sigma_{\text{Co1-O3}} = 0.00$. This further leads to a more pronounced change of the coordination geometry at Co1. The S2 state plays a key role in the catalytic cycle since the oxygen–oxygen bond formation by a water nucleophilic attack is supposed to take place there. As for many other cobalt based WOCs^[50] this reaction is assumed to be rate limiting.^[14,15] Comparing the (canonical) frontier orbitals of the S2 structures of $\{\text{LnCo}_3(\text{OR})_4\}$ we find that in case of the open structure the lowest unoccupied molecular orbitals (LUMOs)+X ($X = 0, 1, \dots, 4$), which are supposed to govern the nucleophilic attack of a water molecule,^[14,15] possess significant contributions of the $\pi_{\text{Co}-\text{O}}^*$ orbitals and the π_{hmp}^* orbitals (see Figures S4 to S7 in SI). How the admixing of the π_{hmp}^* orbitals to the $\pi_{\text{Co}-\text{O}}^*$ orbital could benefit a WNA is not obvious. The most striking difference between the open and closed structure is the stability of the relevant LUMOs. The latter are significantly destabilized in the open form whereas the closed one features energetically low lying accepting orbitals, which in general facilitate the nucleophilic water attack.^[14,15,51] The reactivity of the S2 state is further characterized by the oxo-oxyl resonance,^[52] which in turn is defined by the bond order, and therefore the SEN.^[41,53] In the open structure the SEN between Co1 and its oxo-ligand ($\sigma_{\text{Co}-\text{O}} : 0.43$) is reduced by 21% compared to the closed one ($\sigma_{\text{Co}-\text{O}} : 0.54$), which is in accordance with an elongation of the bond by 0.07 Å. The stronger radical character should potentially enhance the reactivity of the ligand and thereby facilitate the oxygen–oxygen bond formation.^[11] However for a conceptually similar Mn-oxo system, the radical character alone was found not to be crucial for a WNA.^[54]

The energetics of the catalytic intermediates after the WNA shows that the closed structures are always thermodynamically favored compared to the open ones. From a structural point of view those intermediates are again very similar for both catalysts, except for the orientations of the hydroperoxo and hydroxyl ligands. The increased stability of the closed model might (at least partly) originate from an intramolecular hydrogen bond formed between the hydroperoxo ligand and a hydroxyl ligand of the active center (see Figure 2 and Figures S2 and S3 in SI). This, though, may have been favored due to the use of the implicit solvent model COSMO, which has shortcomings with respect to proper inclusion of hydrogen bonding effects.^[55]

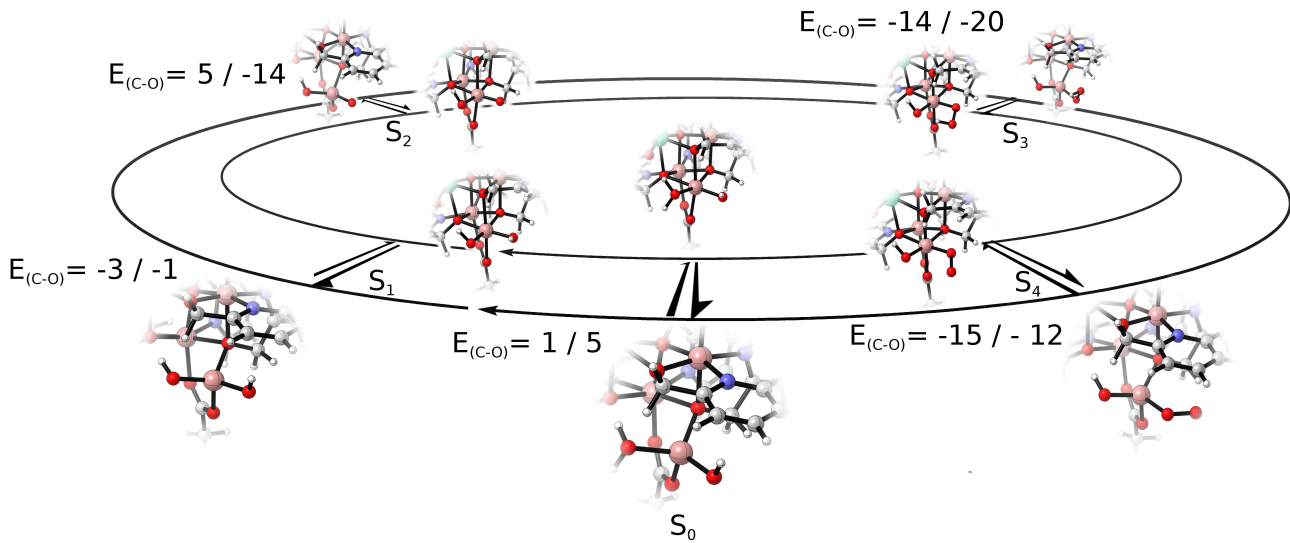


Figure 2. Schematic representation of the catalytic water oxidation mechanism: The inner cycle represents the one based on the previously studied closed cubane core structures^[14] while the outer hosts the catalytic intermediates with an open cubane core. The difference in zero-point-corrected electronic energy between the two conformers is given as $E_{\text{C}-\text{O}} = E_{\text{Closed}} - E_{\text{Open}}$ in kcal/mol (calculated with COSMO). The numbers on the left hand side of the slash correspond to $E_{\text{C}-\text{O}}$ for $\{\text{ErCo}_3(\text{OR})_4\}$, the ones on the right hand side to $\{\text{TmCo}_3(\text{OR})_4\}$. For the sake of clarity only the active center (Co1) and its ligands are shown (see Figures S2 and S3 in SI for complete structures).

The high spin state of the Co1 metal center is energetically favored for all open cubane structures except for the S2 state where the low spin state (in the case of $\{\text{ErCo}_3(\text{OR})_4\}$) and an intermediate spin state (for $\{\text{TmCo}_3(\text{OR})_4\}$) are preferred (see Tables S7 and S8 in SI). However, the different spin states are often within an electronic energy range of less than 5 kcal/mol. The latter is also true for the closed structures (except for the S2 state where the intermediate spin multiplicity leads to a significantly lower electronic energy; see Table S5 in SI). Those findings suggest that multiple spin states are accessible for each intermediate and energetically unfavorable spin-crossing events can be avoided.

The free energy differences between the catalytic intermediates and their respective ground state $\Delta G_{S_i-S_0}$ are given in Figure 3. While $\Delta G_{S_i-S_0}$ for the open and closed structures are similar for the first intermediate (S1), we find that the difference becomes larger along the catalytic pathway.. Those findings bring to mind the relative stability of the intermediates (see Figure 2) and indicate that the open structures do not improve the thermodynamics. The latter is true for both $\{\text{ErCo}_3(\text{OR})_4\}$ and $\{\text{TmCo}_3(\text{OR})_4\}$, since the free energy differences $\Delta G_{S_i-S_0}$ rather increase than decrease compared to the ones of the closed structures.

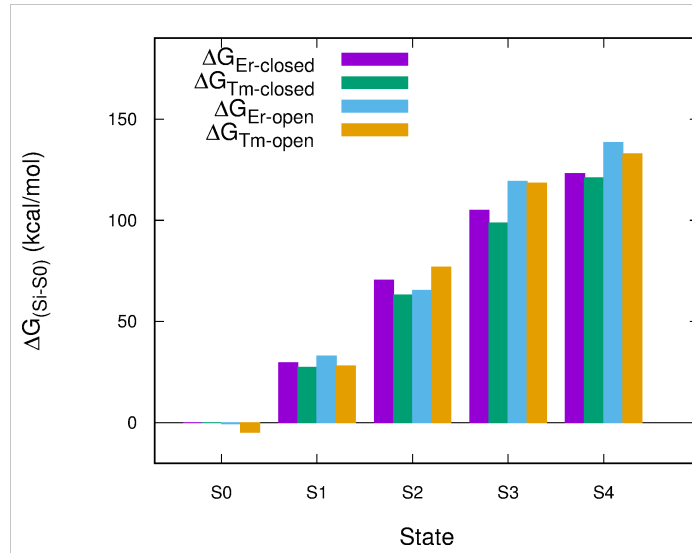


Figure 3. Differences in free energy $\Delta G_{S_i-S_0}$ calculated for $\{\text{ErCo}_3(\text{OR})_4\}$ and $\{\text{TmCo}_3(\text{OR})_4\}$ relative to their catalytic ground state (S0).

This raises the question whether a change from open to close or vice versa is feasible under catalytic conditions. Therefore the energetic barrier for such a structural amendment was calculated in the catalytic ground state (S0) (see Methods for computational details). A possible minimum electronic reaction path for the transition from the closed to the open cubane motif is shown in Figure 4, the electronic energy barrier is estimated to be 6 kcal/mol for both $\{\text{ErCo}_3(\text{OR})_4\}$ and $\{\text{TmCo}_3(\text{OR})_4\}$. The reaction coordinate of both catalysts is highly complex involving multiple bonds and angles. In particular the Co1-O1, and Co1-O3 bonds are elongated during the transition (see SI, Table 11). Further the intramolecular hydrogen bond between the aqua-ligand of Co1 and the hydroxyl of the lanthanide is broken and replaced by a hydrogen bond with O1 (for more details, see Figure S1 in SI).

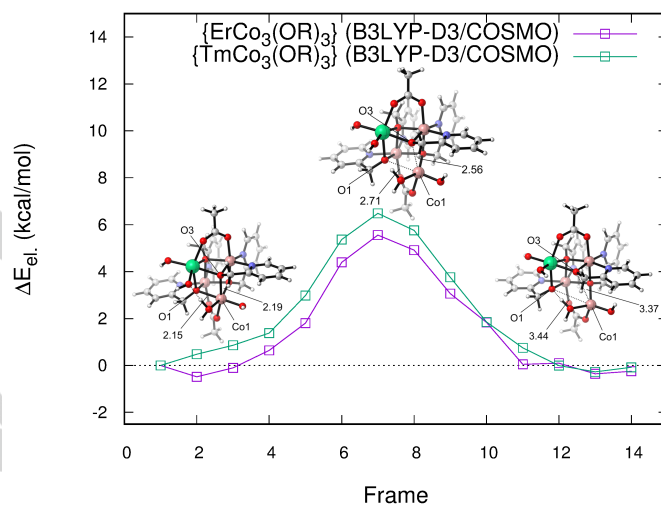


Figure 4. A possible reaction path for the transition from the closed to the open structure in the catalytic ground state (S0) is visualized for both $\{\text{ErCo}_3(\text{OR})_4\}$ and $\{\text{TmCo}_3(\text{OR})_4\}$. The Co1-O1 and Co1-O3 bond lengths are given in Å.

Since the structural change is comparable for all catalytic states, we assume the kinetic barriers to be similar as well. The equilibrium between the two structures is thus mainly driven by their thermodynamics (see Figure 2). The latter suggests that “mixed” cycles composed of both open and closed cubane core structures (see Figure 5) could exist. From the relative stabilities shown in Figure 2 it becomes evident that the open motif may only contribute significantly in the ground state (S0) and the first two intermediates (S1 and S2). In case of $\{\text{ErCo}_3(\text{OR})_4\}$ there are two “mixed” water oxidation pathways (see Tables S12 and S13 in the SI for all reasonable pathways) which either resemble the thermodynamics of an ideal catalyst as good as an all-closed pathway or even slightly better (see Figure 5). A common feature of both “mixed” pathways is the open structure of the catalytic ground state, which however is only slightly more stable than the closed one (about 1 kcal/mol). If the first intermediate also remains in its open form, the pathway becomes slightly unfavorable by 3 kcal/mol, while the open structure in the S2 state again decreases the free energy difference by 5 kcal/mol. If we take all possible combinatorial pathways into account, an open-closed-open-closed-closed pathway is found to resemble an ideal catalyst best. However, such a pathway would require four transitions from open to close cubane core (or vice versa) which – even though the barriers are expected to be reasonably small – is presumably rather unlikely. For $\{\text{TmCo}_3(\text{OR})_4\}$ there is no mixed pathway that is energetically more favorable than the all-closed one. However if solely the first intermediate obtains an open cubane core structure the free energy differences increase by only 5 kcal/mol. In summary the all-closed pathway discussed in detail in Ref. [14] is still the most likely one from a thermodynamic point of view. Nevertheless, our findings strongly suggest that at least for the catalytic ground state (S0) both conformations can coexist.

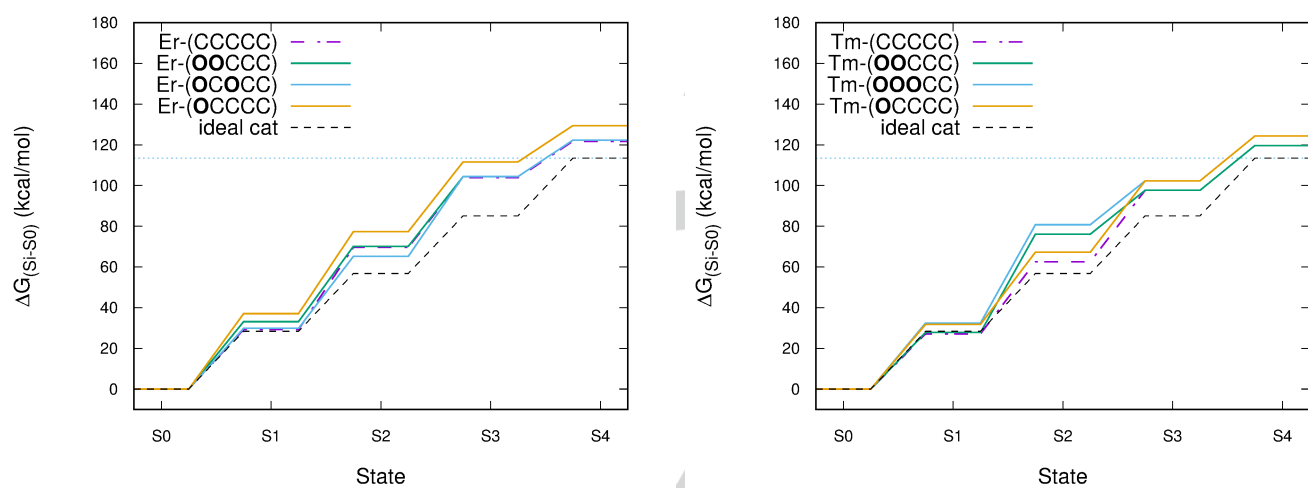


Figure 5. Relative differences in free energy for catalytic cycles composed of O(open) and C(closed) conformers; The horizontal line represents the thermodynamic limit (i.e. the experimental value of 113.5 kcal/mol at pH 0 required for the oxidation of water). Left: Reaction pathways obtained for $\{\text{ErCo}_3(\text{OR})_4\}$; Right: Reaction pathways calculated for $\{\text{TmCo}_3(\text{OR})_4\}$.

In the following section we will address the effects of the solvation model on the different structures.^[56] An inherent problem of many implicit solvent models (such as COSMO) is their inability to accurately describe directed bonds such as hydrogen bonds between solute and solvent. In order to attenuate this limitation, we additionally carried out DCOSMO-RS^[55] calculations (see section Methods). In general the thermodynamics of the open and closed forms are only slightly affected by the use of DCOSMO-RS. Except for the state S2, free energy differences obtained using COSMO and DCOSMO-RS are within 5 kcal/mol (see Tables S4 and S5 in SI). The improved treatment of hydrogen bonding by DCOSMO-RS results in a stabilization of the S2 state by 12 kcal/mol in the case of $\{\text{TmCo}_3(\text{OR})_4\}$ and 9 kcal/mol for $\{\text{ErCo}_3(\text{OR})_4\}$, respectively. The latter is in particular important for the oxo-ligand, which mainly distinguishes the S2 structure from the previous intermediates. The strength of the solute-solvent interaction might be characterized by the surface charge density obtained from COSMO / DCOSMO-RS calculations (see Figure 6). In the case of the open cubane structure, a decrease of the surface charge density at the oxo-ligand is observed when DCOSMO-RS is used instead of COSMO, suggesting weaker interaction between the solvent and the ligand, while for the closed cubane structure the surface charge density is increased at the oxo-ligand implying stronger interactions with the solvent. Relating the weaker solute-solvent interactions in case of the open cubane structure to the oxyl-character of the ligand reveals a reduced hydrophilicity of the oxyl-ligand. Recently it has been reported that the oxyl-ligand^[57] of Ru^V(bda) (bda : 2,2'-bipyridine-6,6'-dicarboxylate) is not susceptible towards hydrogen bonding.^[58] Those findings are in good agreement with the results from the DCOSMO-RS calculations on the S2 state of $\{\text{LnCo}_3(\text{OR})_4\}$.

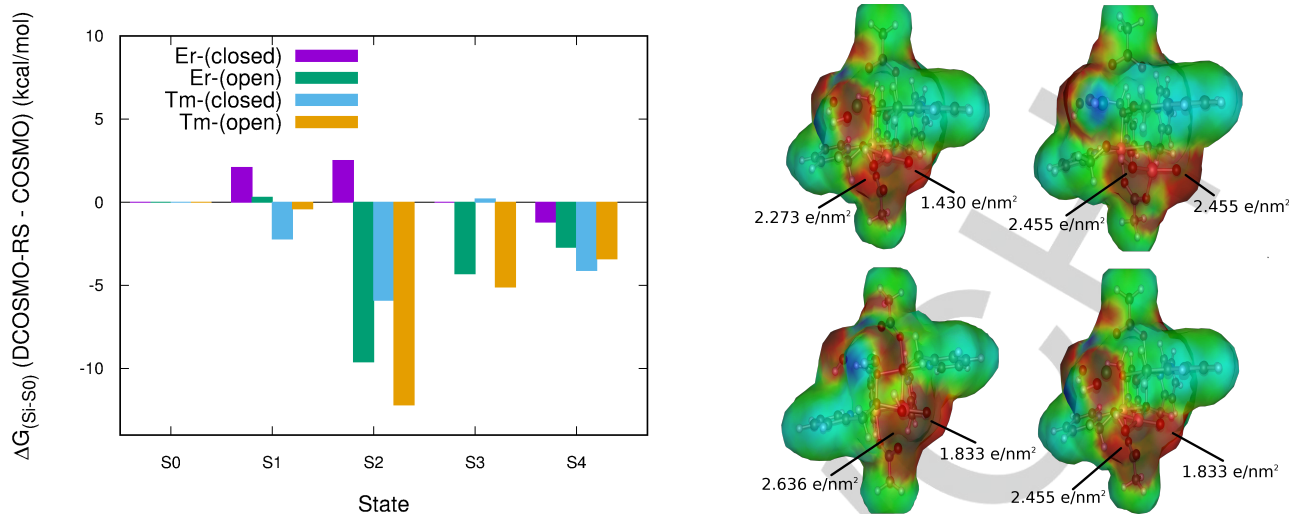


Figure 6. Left: Difference in free energy differences (ΔG_{Si-S0}) obtained employing DCOSMO-RS or COSMO for catalytic water oxidation by $\{\text{ErCo}_3(\text{OR})_4\}$ and $\{\text{TmCo}_3(\text{OR})_4\}$. Right: Surface charge density maps of intermediate S2 ($\{\text{TmCo}_3(\text{OR})_4\}$), obtained by using COSMO (top: closed (left), open (right)) and DCOSMO-RS (bottom: closed (left), open (right)).

Going beyond solvent continuum models in analogy to previous work,^[14,15,56] the structures were also modeled with an explicit first solvation shell derived from a DFT-based MD run (see section Methods for details). A detailed description of the structures can be found in the SI (section “Structural Analysis of Explicit Solvation”). Here, we will only address the important features already discussed in the context of the implicit solvation model. As mentioned earlier, a proper inclusion of solvent-solute interactions is in particular important for the S2 state. When employing explicit solvation, oxo-H distances of ~1.7 Å were found. Such distances are within the range of hydrogen bonds between solvent molecules which are in general between of 1.5 - 1.9 Å. The hydrophilic behavior of the closed cubane core oxo-ligand was already discussed in Ref^[14], where prior to the WNA a proton transfer from the attacking water to another solvent molecule and finally to a hydroxyl ligand of the lanthanide center was observed. The apparently different behavior for conceptually similar catalysts^[58] can easily be resolved since the Co^{III}-oxyl species possess two additional electrons compared to Ru^{IV}-oxyl, which in term increase the basicity of the oxyl-ligand and therefore favor hydrogen bonding. Another consequence of the two electrons is the reduced electrophilicity of the Co^{III}-oxyl that makes a WNA less likely.^[14] Those findings are also in agreement with the COSMO and D-COSMO calculations where the oxyl-ligand was found to be hydrophilic. Another important feature which might be described more accurately using explicit solvation is the formation of intramolecular hydrogen bonds as observed for the state S3. The latter are only observed if the active center (Co1) is in the high-spin state. From an energetic point of view such a high spin configuration is only favorable for $\{\text{TmCo}_3(\text{OR})_4\}$ but not for $\{\text{ErCo}_3(\text{OR})_4\}$. A simplistic interpretation of the correlation between the preferred spin state and the structure of the catalyst is not possible, since the explicit solvation shell has a considerable influence on the orientation of the ligands. Besides structural features, the explicit solvation also influences the stability of the open/closed forms. The latter is measured by the free energy differences $\Delta_{c-o}(\Delta G_{Si-S0})$ (see Tables S1 and S2 in SI). For $\{\text{ErCo}_3(\text{OR})_4\}$, the open form of the states S0 to S2 are stabilized by 18 - 26 kcal/mol compared to the closed ones, while for the S3 and S4 states the closed model is energetically favored. For $\{\text{TmCo}_3(\text{OR})_4\}$, there is an increasing stabilization of the open structure during the catalytic cycle, starting from 6 kcal/mol at the S0 state and reaching almost 30 kcal/mol in the S4 state. Comparing the relative stabilities of the two structural models obtained with implicit and explicit solvation (see Figure 2 and Tables S1 and S2 in SI), we find the open structures to be stabilized by the solvent molecules by 15 - 25 kcal/mol in case of $\{\text{ErCo}_3(\text{OR})_4\}$, and by 2 - 40 kcal/mol in the case of $\{\text{TmCo}_3(\text{OR})_4\}$, respectively. However, it should be kept in mind that the calculation with explicit solvation shell has been carried out within the CP2K package whereas Turbomole was used for the COSMO calculations using different settings (e.g. basis set), which lead to additional differences in the electronic energies. To verify whether the stabilization originates primarily from the hydrogen bonding network within the solvent or from the opening of the cubane cage, we recalculated the electronic energy differences of the cubane structure without solvent molecules (within CP2K). From the absolute differences in free energy $\Delta_{c-o}(\Delta G_{Si-S0})$ it becomes evident that for both catalysts the open structures of the intermediates of the S0 and S1 states are more stable than the closed ones (see Tables S1 and S2 in SI). For the other intermediates, the open and closed forms have either a similar stability or the closed one is energetically favored. There is no consistent trend how the explicit solvation affects the stability of the intermediates in the S2 and S3 states. The lack of a consistent trend might points towards a major disadvantage of a static explicit solvation model. The existence of many shallow local minima on the potential energy surface makes the comparison of energies a tedious task since one has to assure to compare the same local minima with respect to the solvation shell. To get a more accurate description of explicit solvation approaches, sampling methods such as DFT-based MD might be used as described elsewhere.^[56] Nevertheless, such methods are significantly more expensive in terms of computational cost and beyond the scope of this work.

Further, we calculated the barriers for the opening of the $\{\text{LnCo}_3(\text{OR})_4\}$ cubane core in the catalytic ground state (S0) using NEB calculations. Most of the solvent molecules are barely affected by the structural change of the catalyst, only the few molecules close to the active center (Co1) are slightly pushed away from their initial positions due to the opening of the cage. For both catalysts $\{\text{ErCo}_3(\text{OR})_4\}$ and $\{\text{TmCo}_3(\text{OR})_4\}$ electronic barriers of 3.0 kcal/mol were found. The latter are slightly smaller than the ones obtained when employing the implicit solvation model, and emphasize that both the open and closed form of the catalytic ground state can co-exist (see Figure S11 in SI). To compare the relative stability of the intermediates optimized with implicit or explicit solvation directly, electronic energies of the explicitly solvated models were recalculated within TURBOMOLE (with COSMO), where the solvent molecules were deleted. As expected all non-optimized structures are higher in electronic energy than the optimized ones (see Table S3 in SI). However, the free energy differences are for some intermediates as small as 0.3 kcal/mol. This clearly suggests that the open and closed form could coexist for $\{\text{ErCo}_3(\text{OR})_4\}$. In case of $\{\text{TmCo}_3(\text{OR})_4\}$, the explicitly solvated structures are significantly more destabilized compared to the optimized ones by 12 - 30 kcal/mol.

The preferred spin state strongly depends on the solvation model and the used computational settings. For the explicit solvation model (CP2K) (see Tables S6 and S7 in SI), the high spin states are favored for the open model in the S0 and S1 states while for the S2 to S4 states a low spin state on the Co1 metal center is preferred. When the solvent molecules were deleted the trend for the later intermediates inverts (see Table S8 in SI), and we find the intermediates with a high-spin configuration to be energetically favorable. There is a good agreement between the preferred spin states on Co1 for the open structures calculated in TURBOMOLE (with COSMO) and the CP2K structures without explicit solvation, recalculated in TURBOMOLE (with COSMO). Nevertheless, there are no obvious trends with respect to certain spin states for both the two motifs and the two catalysts. The distinct behavior of $\{\text{ErCo}_3(\text{OR})_4\}$ and $\{\text{TmCo}_3(\text{OR})_4\}$ is related to structural differences (see Ref. [14] for a detailed description). The solvation model chosen affects the nuclear and electronic structure, which can change the energetic ordering of the spin states. A more accurate approach beyond DFT would rely on multireference methods, whose application to the highly complex electronic structure of the cubanes presents currently a major challenge, in particular if also solvent effects should be considered.

Conclusion

In summary, we have presented novel structures of the recently presented bioinspired $\{\text{LnCo}_3(\text{OR})_4\}$ ($\text{Ln} = \text{Er}, \text{Tm}$) water oxidation catalysts. Their cubane core can open giving access to a so-called “open” motif. At least for the first two intermediates of the proposed catalytic cycle based on nucleophilic water attack, the two forms (open and closed) are similar from a thermodynamic point of view and kinetically accessible. This further suggests that the “open” cube structures actively contribute towards water oxidation, which is to some extent reminiscent of recent discoveries regarding the OEC.^[45] Comparison of the “open”, “closed” or “mixed” catalytic cycle with the one of a thermodynamically ideal catalyst reveals that in general the “closed” structures better resemble such an ideal catalyst. However, the increased versatility of the coordination geometry of Co1, which may change from octahedral to tetrahedral and vice versa during the water oxidation process, highlights the fact that the ligand environment for those homogeneous catalysts is not completely rigid and therefore might play a crucial role in terms of catalytic activity and long term stability.

The unexpected discovery of the novel structure encouraged us to have a closer look at the influence of the solvation model. When using an explicit solvation shell without applying sampling techniques such as DFT-MD, care has to be taken that the solvation shells resemble the desired local minima. Nevertheless, with an improved description of important solute-solvent interactions structures may be found which would not be detected otherwise. The open cubane core structures initially were only discovered using an explicit solvation model as well. We were also able to prove that they are minima on the potential energy surface using an implicit solvation model. In particular the hydrogen bonding of the solvent and solute appears to play a crucial role in stabilizing certain conformations. Especially the solvation of the oxo-ligand in the S2 state as well as the one of the hydroperoxo ligand in the S3 state have been found to be affected by the solvation model. Employing DCOSMO-RS revealed a significant difference in the description of the oxo-ligand in the “open” and “closed” form compared to the one obtained using COSMO, which might be related to radical character of the oxo-ligand. The hydrophilicity of the latter is expected to directly affect the likelihood for a WNA and is therefore considered to be a key aspect in modeling water oxidation reactions.

Acknowledgements

Funding by Forschungskredit of the University of Zurich, grant. No. FK-15-101, and the Swiss National Science Foundation (grant no. PP00P2_170667) is gratefully acknowledged. We thank the National Center of Competence in Research “Materials Revolution: Computational Design and Discovery of Novel Materials” (NCCR-MARVEL) for support and the Swiss National Supercomputing Center (project ID: s502 and s745) for computing resources. The work has been supported by the University Research Priority Program „Solar Light to Chemical Energy Conversion“ (LightChEC).

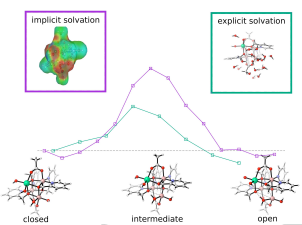
Keywords: water oxidation • computational chemistry • solvation models • cubane

- [1] a) E. Y. Tsui, J. S. Kanady, T. Agapie, *Inorg. Chem.* **2013**, *52*, 13833–13848; b) R. Brimblecombe, A. Koo, G. C. Dismukes, G. F. Swiegers, L. Spiccia, *J. Am. Chem. Soc.* **2010**, *132*, 2892–2894; c) C. Zhang, C. Chen, H. Dong, J.-R. Shen, H. Dau, J. Zhao, *Science* **2015**, *348*, 690–693;
- [2] N. S. McCool, D. M. Robinson, J. E. Sheats, G. C. Dismukes, *J. Am. Chem. Soc.* **2011**, *133*, 11446–11449.
- [3] a) A. M. Ullman, Y. Liu, M. Huynh, D. K. Bediako, H. Wang, B. L. Anderson, D. C. Powers, J. J. Breen, H. D. Abrúñia, D. G. Nocera, *J. Am. Chem. Soc.* **2014**, *136*, 17681–17688; b) A. Genoni, G. La Ganga, A. Volpe, F. Puntoriero, M. Di Valentin, M. Bonchio, M. Natali, A. Sartorel, *Faraday Discuss.* **2015**, *185*, 121–141;
- [4] F. Evangelisti, R. Güttinger, R. Moré, S. Luber, G. R. Patzke, *J. Am. Chem. Soc.* **2013**, *135*, 18734–18737.
- [5] F. Evangelisti, R. Moré, F. Hodel, S. Luber, G. R. Patzke, *J. Am. Chem. Soc.* **2015**, *137*, 11076–11084.
- [6] D. Balcells in *Advances in Organometallic Chemistry*, Elsevier, **2016**.
- [7] a) S. Berardi, G. La Ganga, M. Natali, I. Bazzan, F. Puntoriero, A. Sartorel, F. Scandola, S. Campagna, M. Bonchio, *J. Am. Chem. Soc.* **2012**, *134*, 11104–11107; b) G. La Ganga, F. Puntoriero, S. Campagna, I. Bazzan, S. Berardi, M. Bonchio, A. Sartorel, M. Natali, F. Scandola, *Faraday Discuss.* **2012**, *155*, 177–190;
- [8] J. G. McAlpin, T. A. Stich, C. A. Ohlin, Y. Surendranath, D. G. Nocera, W. H. Casey, R. D. Britt, *J. Am. Chem. Soc.* **2011**, *133*, 15444–15452.
- [9] C. N. Brodsky, R. G. Hadt, D. Hayes, B. J. Reinhart, N. Li, L. X. Chen, D. G. Nocera, *Proc. Natl. Acad. Sci. U. S. A.* **2017**, *114*, 3855–3860.
- [10] P. F. Smith, L. Hunt, A. B. Laursen, V. Sagar, S. Kaushik, K. U. D. Calvinho, G. Marotta, E. Mosconi, F. De Angelis, G. C. Dismukes, *J. Am. Chem. Soc.* **2015**, *137*, 15460–15468.
- [11] X. Li, P. E. M. Siegbahn, *J. Am. Chem. Soc.* **2013**, *135*, 13804–13813.
- [12] L.-P. Wang, T. van Voorhis, *J. Phys. Chem. Lett.* **2011**, *2*, 2200–2204.
- [13] A. Fernando, C. M. Aikens, *J. Phys. Chem. C* **2015**, *119*, 11072–11085.
- [14] F. H. Hodel, S. Luber, *ACS Catal.* **2016**, *6*, 6750–6761.
- [15] F. H. Hodel, S. Luber, *ACS Catal.* **2016**, *6*, 1505–1517.
- [16] J. VandeVondele, M. Krack, F. Mohamed, M. Parrinello, T. Chassaing, J. Hutter, *Comp. Phys. Commun.* **2005**, *167*, 103–128.
- [17] CP2K, Open Source Molecular Dynamics, CP2K Developers Group.
- [18] a) A. D. Becke, *Phys. Rev. A* **1988**, *38*, 3098–3100; b) J. P. Perdew, *Phys. Rev. B* **1986**, *33*, 8822–8824;
- [19] a) A. D. Becke, *The Journal of Chemical Physics* **1993**, *98*, 5648–5652; b) C. Lee, W. Yang, R. G. Parr, *Phys. Rev. B* **1988**, *37*, 785–789; c) M. Guidon, J. Hutter, J. VandeVondele, *J. Chem. Theory. Comput.* **2010**, *6*, 2348–2364;
- [20] a) E. Bill, E. Bothe, P. Chaudhuri, K. Chlopek, D. Herebian, S. Kokatam, K. Ray, T. Weyhermüller, F. Neese, K. Wieghardt, *Chem.* **2004**, *11*, 204–224; b) W. Ames, D. A. Pantazis, V. Krewald, N. Cox, J. Messinger, W. Lubitz, F. Neese, *J. Am. Chem. Soc.* **2011**, *133*, 19743–19757; c) M. Orio, D. A. Pantazis, F. Neese, *Photosyn. Res.* **2009**, *102*, 443–453; d) F. Neese, *J. Biol. Inorg. Chem.* **2006**, *11*, 702–711; e) F. Neese, *Coord. Chem. Rev.* **2009**, *253*, 526–563; f) F. Neese, W. Ames, G. Christian, M. Kampa, D. G. Liakos, D. A. Pantazis, M. Roemelt, P. Surawatanawong, Y. E. Shengfa in *Advances in Inorganic Chemistry*, Elsevier, **2010**;
- [21] K. Kwapien, S. Piccinin, S. Fabris, *J. Phys. Chem. Lett.* **2013**, *4*, 4223–4230.
- [22] M. Reiher, *Inorg. Chem.* **2002**, *41*, 6928–6935.
- [23] a) S. Goedecker, M. Teter, J. Hutter, *Phys. Rev. B* **1996**, *54*, 1703–1710; b) C. Hartwigsen, S. Goedecker, J. Hutter, *Phys. Rev. B* **1998**, *58*, 3641–3662;
- [24] J. VandeVondele, J. Hutter, *The Journal of Chemical Physics* **2007**, *127*, 114105.
- [25] S. Grimme, J. Antony, S. Ehrlich, H. Krieg, *The Journal of Chemical Physics* **2010**, *132*, 154104.
- [26] J. J. Philips, M. A. Hudspeth, P. M. Browne, J. E. Peralta, *Chem. Phys. Lett.* **2010**, *495*, 146–150.
- [27] D. Narzi, D. Bovi, L. Guidoni, *Proc. Natl. Acad. Sci. U. S. A.* **2014**, *111*, 8723–8728.
- [28] J. K. Nørskov, J. Rossmeisl, A. Logadottir, L. Lindqvist, J. R. Kitchin, T. Bligaard, H. Jónsson, *J. Phys. Chem. B* **2004**, *108*, 17886–17892.
- [29] a) S. Piccinin, S. Fabris, *Phys. Chem. Chem. Phys.* **2011**, *13*, 7666–7674; b) Á. Valdés, G.-J. Kroes, *J. Phys. Chem. C* **2010**, *114*, 1701–1708; c) S. Piccinin, A. Sartorel, G. Aquilanti, A. Goldoni, M. Bonchio, S. Fabris, *Proc. Natl. Acad. Sci. U. S. A.* **2013**, *110*, 4917–4922;
- [30] D. R. Stull, H. Prophet, *JANAF Thermochemical Tables*, U.S. National Bureau of Standards, Washington, DC, **1971**.
- [31] G. Henkelman, H. Jónsson, *The Journal of Chemical Physics* **2000**, *113*, 9978–9985.
- [32] G. Henkelman, B. P. Uberuaga, H. Jónsson, *The Journal of Chemical Physics* **2000**, *113*, 9901–9904.
- [33] R. Ahlrichs, M. Bär, M. Häser, H. Horn, C. Kölmel, *Chem. Phys. Lett.* **1989**, *162*, 165–169.
- [34] A. Klamt, G. Schüermann, *J. Chem. Soc., Perkin Trans. 2* **1993**, 799–805.
- [35] F. Weigend, R. Ahlrichs, *Phys. Chem. Chem. Phys.* **2005**, *7*, 3297–3305.
- [36] R. Bauernschmitt, M. Häser, O. Treutler, R. Ahlrichs, *Chem. Phys. Lett.* **1997**, *264*, 573–578.
- [37] F. Weigend, *Phys. Chem. Chem. Phys.* **2006**, *8*, 1057–1065.
- [38] a) P. Deglmann, F. Furche, *The Journal of Chemical Physics* **2002**, *117*, 9535–9538; b) P. Deglmann, F. Furche, R. Ahlrichs, *Chem. Phys. Lett.* **2002**, *362*, 511–518;
- [39] a) F. Eckert, A. Klamt, *AIChE J.* **2002**, *48*, 369–385; b) A. Klamt, V. Jonas, T. Bürger, J. C. W. Lohrenz, *J. Phys. Chem. A* **1998**, *102*, 5074–5085;
- [40] K. Theilacker, D. Bührke, M. Kaupp, *J. Chem. Theory. Comput.* **2015**, *11*, 1111–121.
- [41] C. Ehrhardt, R. Ahlrichs, *Theoret. Chim. Acta* **1985**, *68*, 231–245.
- [42] a) T. A. Halgren, W. N. Lipscomb, *Chem. Phys. Lett.* **1977**, *49*, 225–232; b) R. Elber, M. Karplus, *Chem. Phys. Lett.* **1987**, *139*, 375–380; c) Mills, Jónsson, *Phys. Rev. Lett.* **1994**, *72*, 1124–1127; d) P. Plessow, *J. Chem. Theory. Comput.* **2013**, *9*, 1305–1310;
- [43] W. Humphrey, A. Dalke, K. Schulten, *J. Mol. Graph.* **1996**, *14*, 33–8, 27–8.

- [44] Claude Legault, CYLView, University de Sherbrooke, **2009**.
- [45] N. Cox, M. Retegan, F. Neese, D. A. Pantazis, A. Boussac, W. Lubitz, *Science* **2014**, *345*, 804–808.
- [46] a) H. Isobe, M. Shoji, J.-R. Shen, K. Yamaguchi, *Inorg. Chem.* **2016**, *55*, 502–511; b) V. Krewald, M. Retegan, F. Neese, W. Lubitz, D. A. Pantazis, N. Cox, *Inorg. Chem.* **2016**, *55*, 488–501; c) M. Capone, D. Bovi, D. Narzi, L. Guidoni, *Biochem.* **2015**, *54*, 6439–6442; d) D. A. Pantazis, W. Ames, N. Cox, W. Lubitz, F. Neese, *Angew. Chem. Int. Ed.* **2012**, *51*, 9935–9940;
- [47] M. Retegan, V. Krewald, F. Mamedov, F. Neese, W. Lubitz, N. Cox, D. A. Pantazis, *Chem. Sci.* **2016**, *7*, 72–84.
- [48] M. Amin, L. Vogt, S. Vassiliev, I. Rivalta, M. M. Sultan, D. Bruce, G. W. Brudvig, V. S. Batista, M. R. Gunner, *J. Phys. Chem. B* **2013**, *117*, 6217–6226.
- [49] a) Y. Guo, H. Li, L.-L. He, D.-X. Zhao, L.-D. Gong, Z.-Z. Yang, *Phys. Chem. Chem. Phys.* **2017**, *19*, 13909–13923; b) P. E. M. Siegbahn, *Chem.* **2008**, *14*, 8290–8302;
- [50] a) J. Soriano-López, D. G. Musaev, C. L. Hill, J. R. Galán-Mascarós, J. J. Carbó, J. M. Poblet, *J. Catal.* **2017**, *350*, 56–63; b) M. Z. Ertem, C. J. Cramer, *Dalton Trans.* **2012**, *41*, 12213–12219; c) D. W. Crandell, S. Ghosh, C. P. Berlinguet, M.-H. Baik, *ChemSusChem* **2015**, *8*, 844–852;
- [51] M. Schilling, G. R. Patzke, J. Hutter, S. Luber, *J. Phys. Chem. C* **2016**, *120*, 7966–7975.
- [52] J. R. Winkler, H. B. Gray in *Structure and Bonding* (Eds.: D. M. P. Mingos, P. Day, J. P. Dahl), Springer Berlin Heidelberg, Berlin, Heidelberg, **2012**.
- [53] a) M. Reiher, B. A. Hess, D. Sellmann, *Theor. Chem. Acc.* **2001**, *106*, 379–392; b) M. Reiher, B. Kirchner, *J. Phys. Chem. A* **2003**, *107*, 4141–4146;
- [54] D. C. Ashley, M.-H. Baik, *ACS Catal.* **2016**, *6*, 7202–7216.
- [55] A. Klamt, M. Diedenhofen, *J. Phys. Chem. A* **2015**, *119*, 5439–5445.
- [56] F. H. Hodel, P. Deglmann, S. Luber, *J. Chem. Theory. Comput.* **2017**, *13*, 3348–3358.
- [57] J. Nyhlén, L. Duan, B. Åkermark, L. Sun, T. Privalov, *Angew. Chem. Int. Ed.* **2010**, *122*, 1817–1821.
- [58] S. Zhan, D. Mårtensson, M. Purg, S. C. L. Kamerlin, M. S. G. Ahlquist, *Angew. Chem. Int. Ed.* **2017**, *56*, 6962–6965.

FULL PAPER

We report novel open cubane-core structures for $\{\text{LnCo}_3(\text{OR})_4\}$ ($\text{Ln} = \text{Er}$, Tm) water oxidation catalysts and investigate the influence of implicit and explicit solvation on those structures.



Mauro Schilling, Florian H. Hodel and Sandra Luber*

Page No. – Page No.

Discovery of Open Cubane-Core Structures for biomimetic $\{\text{LnCo}_3(\text{OR})_4\}$ Water Oxidation Catalysts.